



LAWRENCE
LIVERMORE
NATIONAL
LABORATORY

Energy Loss and Flow of Heavy Quarks in Au+Au Collisions at $\sqrt{s}=200\text{GeV}$

Ron Soltz, Jennifer Klay, Akitomo Enokizono,
Jason Newby, Mike Heffner, Ed Hartouni

February 27, 2007

Energy Loss and Flow of Heavy Quarks in Au+Au Collisions at $\sqrt{s}=200\text{ GeV}$

Disclaimer

This document was prepared as an account of work sponsored by an agency of the United States Government. Neither the United States Government nor the University of California nor any of their employees, makes any warranty, express or implied, or assumes any legal liability or responsibility for the accuracy, completeness, or usefulness of any information, apparatus, product, or process disclosed, or represents that its use would not infringe privately owned rights. Reference herein to any specific commercial product, process, or service by trade name, trademark, manufacturer, or otherwise, does not necessarily constitute or imply its endorsement, recommendation, or favoring by the United States Government or the University of California. The views and opinions of authors expressed herein do not necessarily state or reflect those of the United States Government or the University of California, and shall not be used for advertising or product endorsement purposes.

Energy Loss and Flow of Heavy Quarks in Au+Au Collisions at $\sqrt{s_{NN}} = 200$ GeV

A. Adare,⁸ S. Afanasiev,²² C. Aidala,⁹ N.N. Ajitanand,⁴⁹ Y. Akiba,^{43,44} H. Al-Bataineh,³⁸ J. Alexander,⁴⁹ A. Al-Jamel,³⁸ K. Aoki,^{28,43} L. Aphecetche,⁵¹ R. Armendariz,³⁸ S.H. Aronson,³ J. Asai,⁴⁴ E.T. Atomssa,²⁹ R. Averbeck,⁵⁰ T.C. Awes,³⁹ B. Azmoun,³ V. Babintsev,¹⁸ G. Baksay,¹⁴ L. Baksay,¹⁴ A. Baldissieri,¹¹ K.N. Barish,⁴ P.D. Barnes,³¹ B. Bassalleck,³⁷ S. Bathe,⁴ S. Batsouli,^{9,39} V. Baublis,⁴² F. Bauer,⁴ A. Bazilevsky,³ S. Belikov,^{3,21} R. Bennett,⁵⁰ Y. Berdnikov,⁴⁶ A.A. Bickley,⁸ M.T. Bjorndal,⁹ J.G. Boissevain,³¹ H. Borel,¹¹ K. Boyle,⁵⁰ M.L. Brooks,³¹ D.S. Brown,³⁸ D. Bucher,³⁴ H. Buesching,³ V. Bumazhnov,¹⁸ G. Bunce,^{3,44} J.M. Burward-Hoy,³¹ S. Butsyk,^{31,50} S. Campbell,⁵⁰ J.-S. Chai,²³ B.S. Chang,⁵⁸ J.-L. Charvet,¹¹ S. Chernichenko,¹⁸ J. Chiba,²⁴ C.Y. Chi,⁹ M. Chiu,^{9,19} I.J. Choi,⁵⁸ T. Chujo,⁵⁵ P. Chung,⁴⁹ A. Churnyn,¹⁸ V. Cianciolo,³⁹ C.R. Clevelin,¹⁶ Y. Cobigo,¹¹ B.A. Cole,⁹ M.P. Comets,⁴⁰ P. Constantin,^{21,31} M. Csanád,¹³ T. Csörgő,²⁵ T. Dahms,⁵⁰ K. Das,¹⁵ G. David,³ M.B. Deaton,¹ K. Dehmelt,¹⁴ H. Delagrangé,⁵¹ A. Denisov,¹⁸ D. d'Enterria,⁹ A. Deshpande,^{44,50} E.J. Desmond,³ O. Dietzsch,⁴⁷ A. Dion,⁵⁰ M. Donadelli,⁴⁷ J.L. Drachenberg,¹ O. Drapier,²⁹ A. Drees,⁵⁰ A.K. Dubey,⁵⁷ A. Durum,¹⁸ V. Dzhordzhadze,^{4,52} Y.V. Efremenko,³⁹ J. Egdemir,⁵⁰ F. Ellinghaus,⁸ W.S. Emam,⁴ A. Enokizono,^{17,30} H. En'yo,^{43,44} B. Espagnon,⁴⁰ S. Esumi,⁵⁴ K.O. Eyser,⁴ D.E. Fields,^{37,44} M. Finger,^{5,22} F. Fleuret,²⁹ S.L. Fokin,²⁷ B. Forestier,³² Z. Fraenkel,⁵⁷ J.E. Frantz,⁹ A. Franz,³ J. Franz,⁵⁰ A.D. Frawley,¹⁵ K. Fujiwara,⁴³ Y. Fukao,^{28,43} S.-Y. Fung,⁴ T. Fusayasu,³⁶ S. Gadrat,³² I. Garishvili,⁵² F. Gastineau,⁵¹ M. Germain,⁵¹ A. Glenn,^{8,52} H. Gong,⁵⁰ M. Gonin,²⁹ J. Gosset,¹¹ Y. Goto,^{43,44} R. Granier de Cassagnac,²⁹ N. Grau,²¹ S.V. Greene,⁵⁵ M. Grosse Perdekamp,^{19,44} T. Gunji,⁷ H.-Å. Gustafsson,³³ T. Hachiya,^{17,43} A. Hadj Henni,⁵¹ C. Haegemann,³⁷ J.S. Haggerty,³ M.N. Hagiwara,¹ H. Hamagaki,⁷ R. Han,⁴¹ H. Harada,¹⁷ E.P. Hartouni,³⁰ K. Haruna,¹⁷ M. Harvey,³ E. Haslum,³³ K. Hasuko,⁴³ R. Hayano,⁷ M. Heffner,³⁰ T.K. Hemmick,⁵⁰ T. Hester,⁴ J.M. Heuser,⁴³ X. He,¹⁶ H. Hiejima,¹⁹ J.C. Hill,²¹ R. Hobbs,³⁷ M. Hohlmann,¹⁴ M. Holmes,⁵⁵ W. Holzmann,⁴⁹ K. Homma,¹⁷ B. Hong,²⁶ T. Horaguchi,^{43,53} D. Hornback,⁵² M.G. Hur,²³ T. Ichihara,^{43,44} K. Imai,^{28,43} M. Inaba,⁵⁴ Y. Inoue,^{45,43} D. Isenhower,¹ L. Isenhower,¹ M. Ishihara,⁴³ T. Isobe,⁷ M. Issah,⁴⁹ A. Isupov,²² B.V. Jacak,⁵⁰ J. Jia,⁹ J. Jin,⁹ O. Jinnouchi,⁴⁴ B.M. Johnson,³ K.S. Joo,³⁵ D. Jouan,⁴⁰ F. Kajihara,^{7,43} S. Kametani,^{7,56} N. Kamihara,^{43,53} J. Kamin,⁵⁰ M. Kaneta,⁴⁴ J.H. Kang,⁵⁸ H. Kanoh,^{43,53} H. Kano,⁴³ T. Kawagishi,⁵⁴ D. Kawall,⁴⁴ A.V. Kazantsev,²⁷ S. Kelly,⁸ A. Khanzadeev,⁴² J. Kikuchi,⁵⁶ D.H. Kim,³⁵ D.J. Kim,⁵⁸ E. Kim,⁴⁸ Y.-S. Kim,²³ E. Kinney,⁸ A. Kiss,¹³ E. Kistenev,³ A. Kiyomichi,⁴³ J. Klay,³⁰ C. Klein-Boesing,³⁴ L. Kochenda,⁴² V. Kochetkov,¹⁸ B. Komkov,⁴² M. Konno,⁵⁴ D. Kotchetkov,⁴ A. Kozlov,⁵⁷ A. Král,¹⁰ A. Kravitz,⁹ P.J. Kroon,³ J. Kubart,^{5,20} G.J. Kunde,³¹ N. Kurihara,⁷ K. Kurita,^{45,43} M.J. Kweon,²⁶ Y. Kwon,^{52,58} G.S. Kyle,³⁸ R. Lacey,⁴⁹ Y.-S. Lai,⁹ J.G. Lajoie,²¹ A. Lebedev,²¹ Y. Le Bornec,⁴⁰ S. Leckey,⁵⁰ D.M. Lee,³¹ M.K. Lee,⁵⁸ T. Lee,⁴⁸ M.J. Leitch,³¹ M.A.L. Leite,⁴⁷ B. Lenzi,⁴⁷ H. Lim,⁴⁸ T. Liška,¹⁰ A. Litvinenko,²² M.X. Liu,³¹ X. Li,⁶ X.H. Li,⁴ B. Love,⁵⁵ D. Lynch,³ C.F. Maguire,⁵⁵ Y.I. Makdisi,³ A. Malakhov,²² M.D. Malik,³⁷ V.I. Manko,²⁷ Y. Mao,^{41,43} L. Mašek,^{5,20} H. Masui,⁵⁴ F. Matathias,^{9,50} M.C. McCain,¹⁹ M. McCumber,⁵⁰ P.L. McGaughey,³¹ Y. Miake,⁵⁴ P. Mikeš,^{5,20} K. Miki,⁵⁴ T.E. Miller,⁵⁵ A. Milov,⁵⁰ S. Mioduszewski,³ G.C. Mishra,¹⁶ M. Mishra,² J.T. Mitchell,³ M. Mitrovski,⁴⁹ A. Morreale,⁴ D.P. Morrison,³ J.M. Moss,³¹ T.V. Moukhanova,²⁷ D. Mukhopadhyay,⁵⁵ J. Murata,^{45,43} S. Nagamiya,²⁴ Y. Nagata,⁵⁴ J.L. Nagle,⁸ M. Naglis,⁵⁷ I. Nakagawa,^{43,44} Y. Nakamiya,¹⁷ T. Nakamura,¹⁷ K. Nakano,^{43,53} J. Newby,³⁰ M. Nguyen,⁵⁰ B.E. Norman,³¹ A.S. Nyanin,²⁷ J. Nystrand,³³ E. O'Brien,³ S.X. Oda,⁷ C.A. Ogilvie,²¹ H. Ohnishi,⁴³ I.D. Ojha,⁵⁵ H. Okada,^{28,43} K. Okada,⁴⁴ M. Oka,⁵⁴ O.O. Omiwade,¹ A. Oskarsson,³³ I. Otterlund,³³ M. Ouchida,¹⁷ K. Ozawa,⁷ R. Pak,³ D. Pal,⁵⁵ A.P.T. Palounek,³¹ V. Pantuev,⁵⁰ V. Papavassiliou,³⁸ J. Park,⁴⁸ W.J. Park,²⁶ S.F. Pate,³⁸ H. Pei,²¹ J.-C. Peng,¹⁹ H. Pereira,¹¹ V. Peresedov,²² D.Yu. Peressounko,²⁷ C. Pinkenburg,³ R.P. Pisani,³ M.L. Purschke,³ A.K. Purwar,^{31,50} H. Qu,¹⁶ J. Rak,^{21,37} A. Rakotozafindrabe,²⁹ I. Ravinovich,⁵⁷ K.F. Read,^{39,52} S. Rembeczki,¹⁴ M. Reuter,⁵⁰ K. Reygers,³⁴ V. Riabov,⁴² Y. Riabov,⁴² G. Roche,³² A. Romana,^{29,*} M. Rosati,²¹ S.S.E. Rosendahl,³³ P. Rosnet,³² P. Rukoyatkin,²² V.L. Rykov,⁴³ S.S. Ryu,⁵⁸ B. Sahlmueller,³⁴ N. Saito,^{28,43,44} T. Sakaguchi,^{3,7,56} S. Sakai,⁵⁴ H. Sakata,¹⁷ V. Samsonov,⁴² H.D. Sato,^{28,43} S. Sato,^{3,24,54} S. Sawada,²⁴ J. Seele,⁸ R. Seidl,¹⁹ V. Semenov,¹⁸ R. Seto,⁴ D. Sharma,⁵⁷ T.K. Shea,³ I. Shein,¹⁸ A. Shevel,^{42,49} T.-A. Shibata,^{43,53} K. Shigaki,¹⁷ M. Shimomura,⁵⁴ T. Shohjoh,⁵⁴ K. Shoji,^{28,43} A. Sickles,⁵⁰ C.L. Silva,⁴⁷ D. Silvermyr,³⁹ C. Silvestre,¹¹ K.S. Sim,²⁶ C.P. Singh,² V. Singh,² S. Skutnik,²¹ M. Slunečka,^{5,22} W.C. Smith,¹ A. Soldatov,¹⁸ R.A. Soltz,³⁰ W.E. Sondheim,³¹ S.P. Sorensen,⁵² I.V. Sourikova,³ F. Staley,¹¹ P.W. Stankus,³⁹ E. Stenlund,³³ M. Stepanov,³⁸ A. Ster,²⁵ S.P. Stoll,³ T. Sugitate,¹⁷ C. Suire,⁴⁰ J.P. Sullivan,³¹ J. Sziklai,²⁵ T. Tabaru,⁴⁴ S. Takagi,⁵⁴ E.M. Takagui,⁴⁷ A. Taketani,^{43,44} K.H. Tanaka,²⁴ Y. Tanaka,³⁶ K. Tanida,^{43,44} M.J. Tannenbaum,³ A. Taranenko,⁴⁹ P. Tarján,¹²

T.L. Thomas,³⁷ M. Togawa,^{28,43} A. Toia,⁵⁰ J. Tojo,⁴³ L. Tomášek,²⁰ H. Torii,⁴³ R.S. Towell,¹ V-N. Tram,²⁹
 I. Tserruya,⁵⁷ Y. Tsuchimoto,^{17,43} S.K. Tuli,² H. Tydesjö,³³ N. Tyurin,¹⁸ C. Vale,²¹ H. Valle,⁵⁵ H.W. van Hecke,³¹
 J. Velkovska,⁵⁵ R. Vertesi,¹² A.A. Vinogradov,²⁷ M. Virius,¹⁰ V. Vrba,²⁰ E. Vznuzdaev,⁴² M. Wagner,^{28,43}
 D. Walker,⁵⁰ X.R. Wang,³⁸ Y. Watanabe,^{43,44} J. Wessels,³⁴ S.N. White,³ N. Willis,⁴⁰ D. Winter,⁹ C.L. Woody,³
 M. Wysocki,⁸ W. Xie,^{4,44} Y. Yamaguchi,⁵⁶ A. Yanovich,¹⁸ Z. Yasin,⁴ J. Ying,¹⁶ S. Yokkaichi,^{43,44} G.R. Young,³⁹
 I. Younus,³⁷ I.E. Yushmanov,²⁷ W.A. Zajc,^{9,†} O. Zaudtke,³⁴ C. Zhang,^{9,39} S. Zhou,⁶ J. Zimányi,^{25,*} and L. Zolin²²

(PHENIX Collaboration)

¹Abilene Christian University, Abilene, TX 79699, U.S.

²Department of Physics, Banaras Hindu University, Varanasi 221005, India

³Brookhaven National Laboratory, Upton, NY 11973-5000, U.S.

⁴University of California - Riverside, Riverside, CA 92521, U.S.

⁵Charles University, Ovocný trh 5, Praha 1, 116 36, Prague, Czech Republic

⁶China Institute of Atomic Energy (CIAE), Beijing, People's Republic of China

⁷Center for Nuclear Study, Graduate School of Science, University of Tokyo, 7-3-1 Hongo, Bunkyo, Tokyo 113-0033, Japan

⁸University of Colorado, Boulder, CO 80309, U.S.

⁹Columbia University, New York, NY 10027 and Nevis Laboratories, Irvington, NY 10533, U.S.

¹⁰Czech Technical University, Zikova 4, 166 36 Prague 6, Czech Republic

¹¹Dapnia, CEA Saclay, F-91191, Gif-sur-Yvette, France

¹²Debrecen University, H-4010 Debrecen, Egyetem tér 1, Hungary

¹³ELTE, Eötvös Loránd University, H - 1117 Budapest, Pázmány P. s. 1/A, Hungary

¹⁴Florida Institute of Technology, Melbourne, FL 32901, U.S.

¹⁵Florida State University, Tallahassee, FL 32306, U.S.

¹⁶Georgia State University, Atlanta, GA 30303, U.S.

¹⁷Hiroshima University, Kagamiyama, Higashi-Hiroshima 739-8526, Japan

¹⁸IHEP Protvino, State Research Center of Russian Federation, Institute for High Energy Physics, Protvino, 142281, Russia

¹⁹University of Illinois at Urbana-Champaign, Urbana, IL 61801, U.S.

²⁰Institute of Physics, Academy of Sciences of the Czech Republic, Na Slovance 2, 182 21 Prague 8, Czech Republic

²¹Iowa State University, Ames, IA 50011, U.S.

²²Joint Institute for Nuclear Research, 141980 Dubna, Moscow Region, Russia

²³KAERI, Cyclotron Application Laboratory, Seoul, South Korea

²⁴KEK, High Energy Accelerator Research Organization, Tsukuba, Ibaraki 305-0801, Japan

²⁵KFKI Research Institute for Particle and Nuclear Physics of the Hungarian Academy of Sciences (MTA KFKI RMKI), H-1525 Budapest 114, POBox 49, Budapest, Hungary

²⁶Korea University, Seoul, 136-701, Korea

²⁷Russian Research Center "Kurchatov Institute", Moscow, Russia

²⁸Kyoto University, Kyoto 606-8502, Japan

²⁹Laboratoire Leprince-Ringuet, Ecole Polytechnique, CNRS-IN2P3, Route de Saclay, F-91128, Palaiseau, France

³⁰Lawrence Livermore National Laboratory, Livermore, CA 94550, U.S.

³¹Los Alamos National Laboratory, Los Alamos, NM 87545, U.S.

³²LPC, Université Blaise Pascal, CNRS-IN2P3, Clermont-Fd, 63177 Aubiere Cedex, France

³³Department of Physics, Lund University, Box 118, SE-221 00 Lund, Sweden

³⁴Institut für Kernphysik, University of Muenster, D-48149 Muenster, Germany

³⁵Myongji University, Yongin, Kyonggido 449-728, Korea

³⁶Nagasaki Institute of Applied Science, Nagasaki-shi, Nagasaki 851-0193, Japan

³⁷University of New Mexico, Albuquerque, NM 87131, U.S.

³⁸New Mexico State University, Las Cruces, NM 88003, U.S.

³⁹Oak Ridge National Laboratory, Oak Ridge, TN 37831, U.S.

⁴⁰IPN-Orsay, Université Paris Sud, CNRS-IN2P3, BP1, F-91406, Orsay, France

⁴¹Peking University, Beijing, People's Republic of China

⁴²PNPI, Petersburg Nuclear Physics Institute, Gatchina, Leningrad region, 188300, Russia

⁴³RIKEN, The Institute of Physical and Chemical Research, Wako, Saitama 351-0198, Japan

⁴⁴RIKEN BNL Research Center, Brookhaven National Laboratory, Upton, NY 11973-5000, U.S.

⁴⁵Physics Department, Rikkyo University, 3-34-1 Nishi-Ikebukuro, Toshima, Tokyo 171-8501, Japan

⁴⁶Saint Petersburg State Polytechnic University, St. Petersburg, Russia

⁴⁷Universidade de São Paulo, Instituto de Física, Caixa Postal 66318, São Paulo CEP05315-970, Brazil

⁴⁸System Electronics Laboratory, Seoul National University, Seoul, South Korea

⁴⁹Chemistry Department, Stony Brook University, Stony Brook, SUNY, NY 11794-3400, U.S.

⁵⁰Department of Physics and Astronomy, Stony Brook University, SUNY, Stony Brook, NY 11794, U.S.

⁵¹SUBATECH (Ecole des Mines de Nantes, CNRS-IN2P3, Université de Nantes) BP 20722 - 44307, Nantes, France

⁵²University of Tennessee, Knoxville, TN 37996, U.S.

⁵³Department of Physics, Tokyo Institute of Technology, Oh-okayama, Meguro, Tokyo 152-8551, Japan

⁵⁴Institute of Physics, University of Tsukuba, Tsukuba, Ibaraki 305, Japan

⁵⁵*Vanderbilt University, Nashville, TN 37235, U.S.*

⁵⁶*Waseda University, Advanced Research Institute for Science and Engineering, 17 Kikui-cho, Shinjuku-ku, Tokyo 162-0044, Japan*

⁵⁷*Weizmann Institute, Rehovot 76100, Israel*

⁵⁸*Yonsei University, IPAP, Seoul 120-749, Korea*

(Dated: November 29, 2006)

The PHENIX experiment at the Relativistic Heavy Ion Collider (RHIC) has measured electrons with $0.3 < p_{rmT} < 9$ GeV/ c at midrapidity ($|y| < 0.35$) from heavy flavor (charm and bottom) decays in Au+Au collisions at $\sqrt{s_{NN}} = 200$ GeV. The nuclear modification factor R_{AA} relative to $p+p$ collisions shows a strong suppression in central Au+Au collisions, indicating substantial energy loss of heavy quarks in the medium produced at RHIC energies. A large azimuthal anisotropy, v_2 , with respect to the reaction plane is observed for $0.5 < p_{rmT} < 5$ GeV/ c indicating non-zero heavy flavor elliptic flow. A simultaneous description of $R_{AA}(p_{rmT})$ and $v_2(p_{rmT})$ constrains the existing models of heavy-quark rescattering in strongly interacting matter and provides information on the transport properties of the produced medium. In particular, a viscosity to entropy density ratio close to the conjectured quantum lower bound, *i.e.* near a perfect fluid, is suggested.

PACS numbers: 25.75.Dw

Experimental results from the Relativistic Heavy Ion Collider (RHIC) have established that dense partonic matter is formed in Au+Au collisions at RHIC [1, 2, 3, 4]. Strong suppression observed for π^0 and other light hadrons at high transverse momentum (p_{rmT}) [5, 6, 7, 8] indicates partonic energy loss in the produced medium. The azimuthal anisotropy $v_2(p_{rmT})$ [9, 10] provides evidence that collective motion develops in a very early stage of the collision ($\tau \lesssim 5$ fm/ c), in accordance with hydrodynamical calculations [11, 12]. The comparison of v_2 with several such models suggests [13, 14, 15] that the matter formed at RHIC is a near-perfect fluid with viscosity to entropy density ratio η/s close to the conjectured quantum lower bound [16]. Energy loss and flow are related to the transport properties of the medium at temperature T , in particular the diffusion coefficient $D \propto \eta/(sT)$.

Further insight into properties of the produced medium can be gained from the production and propagation of particles carrying heavy quarks (charm or bottom). A fixed-order-plus-next-to-leading-log (FONLL) pQCD calculation [17] describes the cross sections of heavy-flavor decay electrons in $p+p$ collisions at $\sqrt{s} = 200$ GeV within theoretical uncertainties [18]. In Au+Au collisions the total yield of heavy-flavor decay electrons was found to scale with the number of nucleon-nucleon collisions as expected for point-like processes [19]. Energy loss via gluon radiation is expected to be reduced for quarks with larger mass at moderate p_T due to suppression of forward radiation, thus increasing the expected thermalization time [20, 21, 22]. Consequently, a decrease of high p_T suppression and of v_2 is expected from light to charm to bottom quarks, with the absolute values and their p_T dependence being sensitive to the properties of the medium. In contrast to these expectations a strong suppression of heavy-flavor decay electrons was discovered at high p_{rmT} [23], going together with nonzero electron v_2 at intermediate p_{rmT} [24]. Recently, other measurements for $p+p$ and Au+Au collisions were reported [25].

This Letter presents p_T spectra and the elliptic flow amplitude v_2^{HF} of electrons, $(e^+ + e^-)/2$, from heavy-flavor decays at midrapidity in Au+Au collisions at $\sqrt{s_{NN}} = 200$ GeV. The much higher statistics and reduced systematic uncertainties compared to earlier data [19, 23, 24] permit a determination of the centrality dependence of R_{AA} in an extended p_T range ($p_{rmT} < 9$ GeV/ c) and a measurement of v_2^{HF} for $p_{rmT} < 5$ GeV/ c .

The data were collected by the PHENIX detector [26] in the 2004 RHIC run. The minimum bias trigger and the collision centrality were obtained from the beam-beam counters (BBC) and zero degree calorimeters [1]. After selecting good runs, data samples of 8.1 and 7.0×10^8 minimum bias events in the vertex range $|z_{\text{vtx}}| < 20$ cm are used for the spectra and v_2 analyses, respectively.

Charged particle tracks are reconstructed with the two PHENIX central arm spectrometers, each covering $\Delta\phi = \pi/2$ in azimuth and $|\eta| < 0.35$ in pseudorapidity [26]. Tracks are confirmed by matching showers in the electromagnetic calorimeter (EMCal) within 2σ in position. Electron candidates have at least three associated hits in the ring imaging Čerenkov detectors (RICH) and fulfill a shower shape cut in the EMCal, where they deposit an energy, E , consistent with the momentum ($E/p - 1 > -2\sigma$). Below the Čerenkov threshold for pions ($p_{rmT} < 5$ GeV/ c) electron mis-identification is only due to random coincidences between hadron tracks and hits in the RICH. This small background ($< 20\%$ at low p_T in central collisions, less towards high p_T and peripheral events) is subtracted statistically using an event mixing technique. Requiring at least five hits in the RICH and tightening the shower shape cut extends the electron measurement to 9 GeV/ c in p_{rmT} , with negligible hadron background for $p_{rmT} < 8$ GeV/ c and a hadron contamination of 20% for $8 < p_{rmT} < 9$ GeV/ c . The raw spectra are corrected for geometrical acceptance and reconstruction efficiency determined by a GEANT simulation. The

centrality dependent efficiency loss $< 2\%$ ($\approx 23\%$) for peripheral (central) events is evaluated by reconstructing simulated electrons embedded into real events.

The inclusive electron spectra consist of (1) “non-photon” electrons from heavy-flavor decays, (2) “photon” background from Dalitz decays and photon conversions (mainly in the beam pipe), and (3) “non-photon” background from $K \rightarrow e\pi\nu$ (K_{e3}) and dielectron decays of vector mesons. Contribution (3) is small ($< 10\%$ for $p_{rmT} < 0.5$ GeV/ c , $< 2\%$ for $p_{rmT} > 2$ GeV/ c) compared to (2). The heavy-flavor signal and the ratio of non-photon to photon electrons, R_{NP} , is determined via two independent and complementary methods.

Both methods are described in detail in [18], where the identical detector configuration was used. At low p_{rmT} ($p_{rmT} < 1.6$ GeV/ c), where the heavy-flavor signal to background ratio is small ($S/B \ll 1$), the “converter subtraction” method is used which employs a photon converter of 1.67% radiation length (X_0) installed around the beam pipe for part of the run. The converter multiplies the photonic background by an almost p_T independent factor $R_\gamma \sim 2.3$. The photonic background can then be determined by comparing the inclusive electron yield with and without the converter. For higher p_{rmT} , where S/B is large, the “cocktail subtraction” method [23] is used. Here the background is calculated with a Monte Carlo hadron decay generator and subtracted from the data. At low p_T the dominant background source is the π^0 Dalitz decay, which is calculated for each centrality using measured pion spectra [6, 27] as input. In good agreement with measured data [8], the spectral shapes of other light hadrons h (η , ρ , ω , ϕ , η') are derived from the pion spectrum assuming a universal shape in $m_T = \sqrt{p_{rmT}^2 + m_h^2}$ with a fixed constant ratio at high p_{rmT} . Photon conversions in the beam pipe, air and helium bags (total: $0.4\% X_0$) are also included, along with background from K_{e3} decays and both external and internal conversions of direct photons which are important for $p_{rmT} > 4$ GeV/ c . The agreement within the systematic uncertainties in the overlap region $0.3 < p_{rmT} < 4$ GeV/ c of these two methods demonstrates that the absolute value of photonic backgrounds in the PHENIX aperture is well-understood.

The v_2 of inclusive electrons, v_2^{inc} , is measured as $v_2^{inc} = \langle \cos(2(\phi - \Phi_R)) \rangle / \sigma_R$ [28], where Φ_R is the azimuthal orientation of the reaction plane measured with the resolution σ_R using the BBC [9]. Since σ_R is centrality dependent, v_2 is determined for narrow centrality bins (10%) and then averaged to calculate v_2 for minimum bias events. The v_2 of random hadronic background is subtracted statistically as described in [24].

The $v_2^{non-\gamma}$ of non-photon electrons is obtained by subtracting the photonic electron v_2^γ as: $v_2^{non-\gamma} = ((1 + R_{NP})v_2^{inc} - v_2^\gamma) / R_{NP}$. Here v_2^γ is calculated via a Monte Carlo generator that includes π^0 , η , and direct photons. The measured $v_2(p_{rmT})$ of π^\pm, π^0 and K^\pm [9, 29]

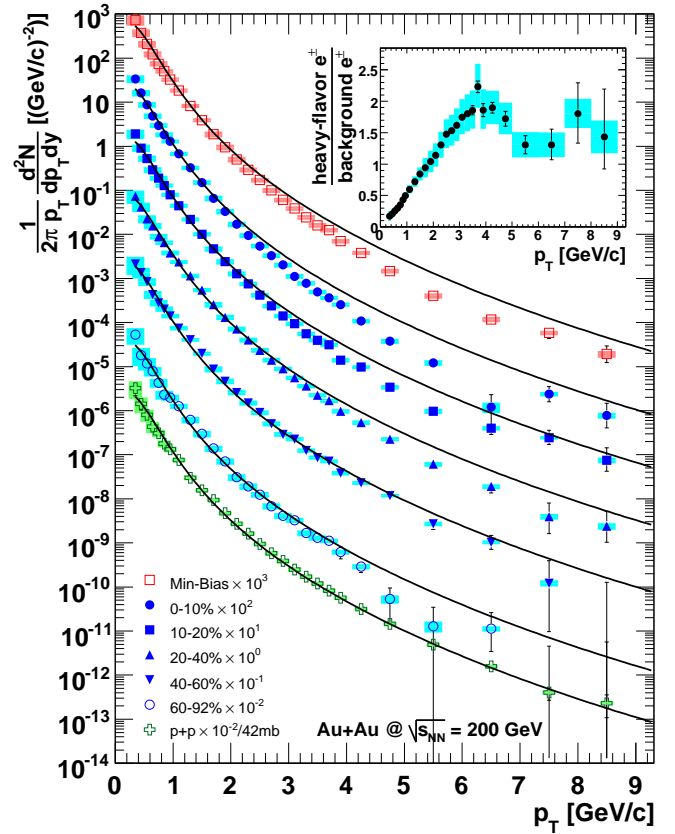


FIG. 1: Invariant yields of electrons from heavy-flavor decays for different Au+Au centrality classes and for $p+p$ collisions, scaled by powers of ten for clarity. The solid lines are the result of a FONLL calculation normalized to the $p+p$ data [18] and scaled with $\langle T_{AA} \rangle$ for each Au+Au centrality class. The insert shows the ratio of heavy-flavor to background electrons for minimum bias Au+Au collisions. Error bars (boxes) depict statistical (systematic) uncertainties.

is used as input, assuming $v_2^{\pi^\pm} = v_2^{\pi^0}$, $v_2^\eta = v_2^{K^\pm}$, and $v_2^{\text{direct}\gamma} = 0$. A direct measurement of v_2^γ using the converter subtraction method confirms the calculation within statistical uncertainties. The resulting $v_2^{non-\gamma}$ has a small contribution from K_{e3} background which is simulated and subtracted to obtain v_2^{HF} of heavy-flavor decay electrons.

Three independent categories of systematic uncertainties are considered. (A) Systematic errors in the inclusive electron spectra include uncertainties in the geometrical acceptance (5%), the reconstruction efficiency (3%), and the embedding correction ($\leq 4\%$). (B) Uncertainties in the converter subtraction are mainly given by the uncertainty in R_γ (2.7%) and in the relative acceptance of runs with and without the converter being installed (1%). (C) Uncertainties in the cocktail subtraction rise from 8% at $p_{rmT} = 0.3$ GeV/ c to 13% at 9 GeV/ c , dominated by systematic errors in the pion input and, at high p_{rmT} , the direct photon spectrum. For the v_2 measurement a systematic uncertainty of 5% due to the reaction plane

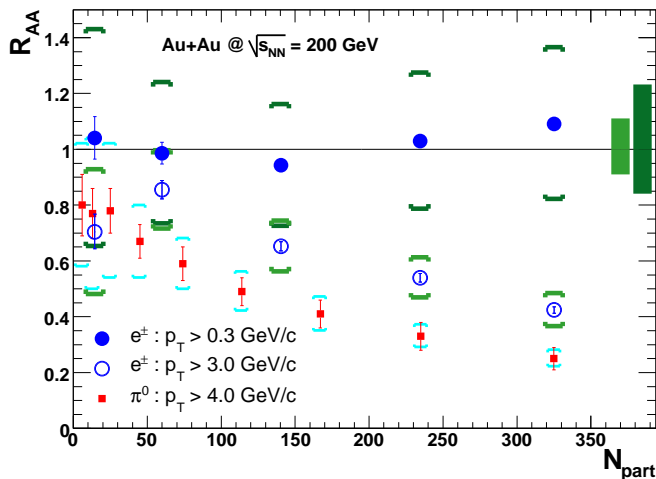


FIG. 2: R_{AA} of heavy-flavor electrons with p_T above 0.3 and 3 GeV/c and of π^0 with $p_{rmT} > (4 \text{ GeV}/c)$ as function of centrality given by N_{part} . Error bars (brackets) depict statistical (point-by-point systematic) uncertainties. The right (left) box at $R_{AA} = 1$ shows the relative uncertainty from the $p+p$ reference common to all points for $p_{rmT} > 0.3(3) \text{ GeV}/c$.

measurement is added for minimum bias events.

Figure 1 shows the invariant p_T spectra of electrons from heavy-flavor decay for minimum bias events and in five centrality classes. The curves overlaid are the fit to the corresponding data from $p+p$ collisions [18] with the spectral shape taken from a FONLL calculation [17] and scaled by the nuclear overlap integral $\langle T_{AA} \rangle$ for each centrality class [6]. The insert in Fig. 1 shows the ratio of electrons from heavy-flavor decays to background. It increases rapidly with p_{rmT} , reaching one for $p_{rmT} \approx 1.5 \text{ GeV}/c$, reflecting the small amount of material in the detector acceptance. It is this large signal to background ratio which makes the accurate measurement of heavy-flavor electron spectra and v_2^{HF} possible.

For all centralities, the Au+Au spectra agree well with the $p+p$ reference at low p_T but a suppression with respect to $p+p$ develops towards high p_{rmT} . This is quantified by the nuclear modification factor $R_{AA} = dN_{Au+Au}/(\langle T_{AA} \rangle d\sigma_{p+p})$, where dN_{Au+Au} is the differential yield in Au+Au and $d\sigma_{p+p}$ is the differential cross section in $p+p$ in a given p_T bin. For $p_{rmT} < 1.6 \text{ GeV}/c$, $d\sigma_{p+p}$ is taken bin-by-bin from [18], whereas a fit to the same data (curves in Fig. 1) is used at higher p_{rmT} , taking the normalization uncertainty into account. Systematic uncertainties in $d\sigma_{p+p}$ and T_{AA} are included.

Figure 2 shows R_{AA} for electrons from heavy-flavor decays for two different p_T ranges as a function of the number of participant nucleons, N_{part} . For $p_{rmT} > 0.3 \text{ GeV}/c$, which contains more than half of the heavy-flavor decay electrons [18], R_{AA} is close to unity for all N_{part} in accordance with the binary scaling of the total heavy-flavor yield [19]. For $p_{rmT} > 3 \text{ GeV}/c$, the heavy flavor electron R_{AA} decreases systematically

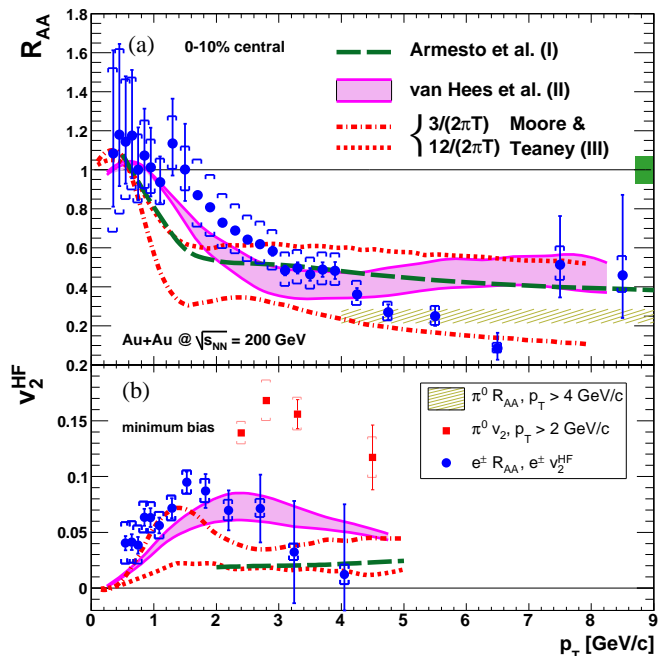


FIG. 3: (a) R_{AA} of heavy-flavor electrons in 0-10% central collisions compared with π^0 data [6] and model calculations (curves I [30], II [31], and III [32]). The box at $R_{AA} = 1$ shows the uncertainty in T_{AA} . (b) v_2^{HF} of heavy-flavor electrons in minimum bias collisions compared with π^0 data [29] and the same models. Errors are shown as in Fig. 2.

with centrality, and it is larger than R_{AA} of π^0 with $p_{rmT} > 4 \text{ GeV}/c$ [6]. Since above 3 GeV/c electrons from charm decays originate mainly from D mesons with p_T above 4 GeV/c this comparison indicates a slightly smaller high p_T suppression of heavy-flavor mesons than observed for light mesons.

Figure 3 shows the measured R_{AA} and v_2^{HF} of heavy-flavor electrons in 0-10% central and minimum bias collisions, and our corresponding π^0 data [6, 29]. The latter are restricted to p_T ranges where R_{AA} and v_2 of π^0 do not depend strongly on p_T such that a comparison of heavy-flavor electrons and π^0 is not obscured by decay kinematics. The data indicate strong coupling of heavy quarks to the medium. The suppression is large and similar to that of π^0 for $p_{rmT} > 4 \text{ GeV}/c$ where a significant contribution from bottom decays is expected. The large v_2^{HF} shows that the charm relaxation time is comparable to the short time scale of flow development in the produced medium.

More quantitative statements require theoretical guidance. Figure 3 compares the R_{AA} and v_2 of heavy-flavor electrons with models calculating both quantities simultaneously. A perturbative QCD calculation with radiative energy loss (curves I) [30] can describe the measured R_{AA} reasonably well using a large transport coefficient $\hat{q} = 14 \text{ GeV}^2/\text{fm}$, which leads to a consistent description of light hadron suppression as well. This value of \hat{q}

would imply a strongly coupled medium. The azimuthal anisotropy is only due to the path length dependence of energy loss in this model, and the data clearly favor larger v_2^{HF} than predicted from this effect alone.

Figure 3 also shows that the large v_2^{HF} is better reproduced in Langevin-based heavy quark transport calculations [31, 32]. A calculation which includes elastic scattering mediated by resonance excitation (curves II) [31] is in good simultaneous agreement with the measured R_{AA} and v_2 . This is achieved with a small heavy quark relaxation time τ which translates into a diffusion coefficient $D_{HQ} \times (2\pi T) = 4 - 6$ in this model [31]. Energy loss and flow are calculated in terms of D_{HQ} as well (curves III) in [32]. While this model fails to describe the measured R_{AA} and v_2 simultaneously with one value for D_{HQ} the range for D_{HQ} that leads to reasonable agreement with R_{AA} or v_2 is similar to the estimate from [31]. These calculations suggest that small τ and/or $D_{HQ} \times (2\pi T)$ are required to reproduce the data. Note that D_{HQ} provides an upper bound for the bulk matter's diffusion coefficient D which in turn is related to the viscosity to entropy ratio η/s . Intriguingly, the values for D used in [31, 32] correspond to small values of η/s at or near the conjectured quantum bound $1/4\pi$ [33]. This observation is consistent with estimates obtained in the light quark sector from elliptic flow [34] and fluctuation analyses [35].

The conjecture of a bound on η/s [16] was obtained using the AdS/CFT correspondence [36, 37], which exploits a duality between strongly coupled gauge theories and semiclassical gravitational physics. Recently, such methods were applied to estimate D_{HQ} in a thermalized plasma [38, 39, 40]. These authors also find a small diffusion coefficient $D_{HQ} \times (2\pi T) \sim 1$.

In conclusion, we have observed large energy loss and flow of heavy quarks in Au+Au collisions at $\sqrt{s_{\text{NN}}} = 200$ GeV. The data provide strong evidence for the coupling of heavy quarks to the produced medium. A short relaxation time of heavy quarks and/or a small diffusion coefficient are required by the data, suggesting a viscosity to entropy ratio of the medium close to the quantum lower bound, *i.e.* near a perfect fluid.

We thank the staff of the Collider-Accelerator and Physics Departments at BNL for their vital contributions. We acknowledge support from the Department of Energy and NSF (U.S.A.), MEXT and JSPS (Japan), CNPq and FAPESP (Brazil), NSFC (China), MSMT (Czech Republic), IN2P3/CNRS, and CEA (France), BMBF, DAAD, and AvH (Germany), OTKA (Hungary), DAE (India), ISF (Israel), KRF and KOSEF (Korea), MES, RAS, and FAAE (Russia), VR and KAW (Swe-

den), U.S. CRDF for the FSU, US-Hungarian NSF-OTKA-MTA, and US-Israel BSF.

* Deceased

† PHENIX Spokesperson: zajc@nevis.columbia.edu

- [1] K. Adcox *et al.*, Nucl. Phys. **A757**, 184 (2005).
- [2] I. Arsene *et al.*, Nucl. Phys. **A757**, 1 (2005).
- [3] B. B. Back *et al.*, Nucl. Phys. **A757**, 28 (2005).
- [4] J. Adams *et al.*, Nucl. Phys. **A757**, 102 (2005).
- [5] K. Adcox *et al.*, Phys. Rev. Lett. **88**, 022301 (2002).
- [6] S. S. Adler *et al.*, Phys. Rev. Lett. **91**, 072301 (2003).
- [7] J. Adams *et al.*, Phys. Rev. Lett. **91**, 172302 (2003).
- [8] S. S. Adler *et al.*, Phys. Rev. Lett. **96**, 202301 (2006).
- [9] S. S. Adler *et al.*, Phys. Rev. Lett. **91**, 182301 (2003).
- [10] J. Adams *et al.*, Phys. Rev. Lett. **92**, 052302 (2004).
- [11] P. Huovinen *et al.*, Phys. Lett. **B503**, 58 (2001).
- [12] T. Hirano, M. Gyulassy, Nucl. Phys. **A769**, 71 (2006).
- [13] E. Shuryak, Prog. Part. Nucl. Phys. **53**, 273 (2004).
- [14] M. Gyulassy, L. McLerran, Nucl. Phys. **A750**, 30 (2005).
- [15] P. F. Kolb, U. W. Heinz, nucl-th/0305084.
- [16] P. Kovtun, D. T. Son, A. O. Starinets, Phys. Rev. Lett. **94**, 111601 (2005).
- [17] M. Cacciari *et al.*, Phys. Rev. Lett. **95**, 122001 (2005)
- [18] A. Adare *et al.*, hep-ex/0609010.
- [19] S. S. Adler *et al.*, Phys. Rev. Lett. **94**, 082301 (2005).
- [20] Y. L. Dokshitzer, D. E. Kharzeev, Phys. Lett. **B519**, 199 (2001).
- [21] S. Wicks *et al.*, nucl-th/0512076.
- [22] N. Armesto *et al.*, Phys. Lett. **B637**, 362 (2006).
- [23] S. S. Adler *et al.*, Phys. Rev. Lett. **96**, 032301 (2006).
- [24] S. S. Adler *et al.*, Phys. Rev. **C72**, 024901 (2005).
- [25] B. I. Abelev *et al.*, nucl-ex/0607012.
- [26] K. Adcox *et al.*, Nucl. Instrum. Meth. **A499**, 469 (2003).
- [27] S. S. Adler *et al.*, Phys. Rev. **C69**, 034909 (2004).
- [28] A. M. Poskanzer, S. A. Voloshin, Phys. Rev. **C58**, 1671 (1998).
- [29] S. S. Adler *et al.*, Phys. Rev. Lett. **96**, 032302 (2006).
- [30] N. Armesto, *et al.*, Phys. Lett. **B637**, 362 (2006).
- [31] H. van Hees, V. Greco, R. Rapp, Phys. Rev. **C73**, 034913 (2006) and private communication.
- [32] G. D. Moore, D. Teaney, Phys. Rev. **C71**, 064904 (2005) and private communication.
- [33] Similar estimates of D may be found in J. Casalderrey-Solana, D. Teaney, Phys. Rev. **D74**, 085012 (2006), and E. Shuryak, nucl-th/0609013.
- [34] R. A. Lacey *et al.*, nucl-ex/0609025
- [35] S. Gavin, M. Abdel-Aziz, nucl-th/0606061.
- [36] J. M. Maldacena, Adv. Theor. Math. Phys. **2**, 231 (1998).
- [37] E. Witten, Adv. Theor. Math. Phys. **2**, 505 (1998).
- [38] C. P. Herzog *et al.*, JHEP **0607**, 013 (2006).
- [39] S. S. Gubser, hep-th/0605182.
- [40] J. J. Friess, S. S. Gubser, G. Michalogiorgakis, hep-th/0605292.